

Effect of radio frequency bias on plasma characteristics of inductively coupled argon discharge based on fluid simulations*

Xiao-Yan Sun(孙晓艳)^{1,†}, Yu-Ru Zhang(张钰如)², Sen Chai(柴森)³,
You-Nian Wang(王友年)², Yan-Yan Chu(楚艳艳)¹, and Jian-Xin He(何建新)^{1,‡}

¹Textile and Garment Industry of Research Institute, Zhongyuan University of Technology, Zhengzhou 450007, China

²Key Laboratory of Materials Modification by Laser, Ion, and Electron Beams (Ministry of Education),
School of Physics, Dalian University of Technology, Dalian 116024, China

³China Special Equipment Inspection and Research Institute, Beijing 100029, China

(Received 1 April 2020; revised manuscript received 10 May 2020; accepted manuscript online 19 May 2020)

A fluid model is employed to investigate the effect of radio frequency bias on the behavior of an argon inductively coupled plasma (ICP). In particular, the effects of ICP source power, single-frequency bias power, and dual-frequency bias power on the characteristics of ICP are simulated at a fixed pressure of 30 mTorr (1 Torr = 1.33322×10^2 Pa). When the bias frequency is fixed at 27.12 MHz, the two-dimensional (2D) plasma density profile is significantly affected by the bias power at low ICP source power (*e.g.*, 50 W), whereas it is weakly affected by the bias power at higher ICP source power (*e.g.*, 100 W). When dual-frequency (27.12 MHz/2.26 MHz) bias is applied and the sum of bias powers is fixed at 500 W, a pronounced increase in the maximum argon ion density is observed with the increase of the bias power ratio in the absence of ICP source power. As the ratio of 27.12-MHz/2.26-MHz bias power decreases from 500 W/0 W to 0 W/500 W with the ICP source power fixed at 50 W, the plasma density profiles smoothly shifts from edge-high to center-high, and the effect of bias power on the plasma distribution becomes weaker with the bias power ratio decreasing. Besides, the axial ion flux at the substrate surface is characterized by a maximum at the edge of the substrate. When the ICP source power is higher, the 2D plasma density profiles, as well as the spatiotemporal and radial distributions of ion flux at the substrate surface are characterized by a peak in the reactor center, and the distributions of plasma parameters are negligibly affected by the dual-frequency bias power ratio.

Keywords: fluid simulation, single- and dual-frequency bias power, plasma distribution

PACS: 52.65.-y, 52.50.Qt, 52.30.Ex

DOI: 10.1088/1674-1056/ab9436

1. Introduction

Inductively coupled plasma (ICP) sources are widely used in microelectronics manufacturing industry, *e.g.*, for etching of wafer,^[1] deposition of thin-films,^[2] and ion implantation,^[3] due to the advantages of high-density plasma generation in a simple low-pressure chamber. The bombardment of ions onto a wafer plays a key role in etching and ion implantation process. Thus, an additional radio frequency (RF) bias source is usually employed to control the energy of incident ions. However, it has been observed that the bias power not only determines the ion energy distribution but also influences the plasma properties under the some conditions. Therefore, a clear understanding of the effect of bias power is crucial to controlling the discharge process and to optimizing the plasma for microelectronic applications.

Over the past few years, numerous experimental and theoretical studies have focused on the bias effects in ICP discharges.^[4–16] For instance, Lee *et al.*^[4] experimentally observed that with the increase in the bias power, the plasma density increased near the radial edge and the plasma uniformity

was significantly enhanced at a gas pressure of 50 mTorr. Subsequently, the influence of skin effect on the plasma uniformity was experimentally investigated under RF bias power, and the plasma uniformity was dramatically changed with ICP power varying.^[5] Sobolewski and Kim^[6] found that when bias was applied, the electron density decreased at high ICP powers in Ar, CF₄, and Ar/CF₄ plasma and increased at low ICP power. Ahr *et al.*^[7] experimentally revealed that when the relative phase between the ICP power and the bias power was fixed at 60°, the threshold for the E- to H-mode transition was reduced with the decrease in the bias power. Hoekstra and Kushner^[10] employed a hybrid model to observe a small improvement in the uniformity of ion flux at high RF bias in Ar/Cl₂ discharge. Using the particle-in-cell Monte Carlo method, Takekida and Nanbu^[11] revealed that a uniform ion flux could be obtained by reducing the bias frequency. Tinck *et al.*^[12] used the hybrid plasma equipment model (HPERM) to demonstrate that the ion flux hitting the substrate became higher with bias increasing, thereby increasing the etch rate. Kwon *et al.*^[13] studied the electron densities for different bias power values in an argon discharge both experimentally and theoretically, and they

*Project supported by the National Natural Science Foundation of China (Grant Nos. 11875101 and 11905307).

†Corresponding author. E-mail: xysun@zut.edu.cn

‡Corresponding author. E-mail: hejianxin771117@163.com

© 2020 Chinese Physical Society and IOP Publishing Ltd

<http://iopscience.iop.org/cpb> <http://cpb.iphy.ac.cn>

found that the electron density decreased with bias power increasing in the inductive mode. Gao *et al.*^[14] found an inflexion point of electron density with increasing RF bias voltage in the H mode of ICPs both experimentally and theoretically. Subsequently, Jang and Chae^[16] demonstrated that the ratio of dual-frequency (27.12 MHz/2 MHz) bias power could be used to control the ion energy, and this ratio has a negligible effect on the value of ion density.

Although several studies have focused on the bias effects in ICP discharges, a systematic investigation for revealing the variation in the two-dimensional (2D) spatial distribution of plasma parameters with single-frequency and dual-frequency bias parameters has not been reported yet. Because the distribution of plasma characteristics is vital for controlling the process of semiconductor etching, it is of great interest to elucidate the effect of bias on the plasma distributions. Therefore, in this study, the multi-physics analysis for plasma sources-ICP (MAPS-ICP) solver^[17–21] composed of a fluid module and a sheath module^[22,23] is employed to investigate the effects of single-frequency and dual-frequency bias on the plasma characteristics at different values of ICP source power. Our results provide a useful insight into the effect of source power, which can be used for optimizing the plasma processing techniques.

The rest of this paper is organized as follows. A description of the MAPS-ICP solver is presented in Section 2. The effects of the single-frequency and dual-frequency bias power on the characteristics of argon plasma for various values of ICP source are shown in Section 3. Finally, the important results of the study are summarized in Section 4.

2. Description of MAPS-ICP solver

Figure 1 shows a schematic of the ICP chamber used in this work. The radius and height of the chamber are 22.0 cm and 9 cm, respectively. The bottom electrode is placed 7 cm away from the quartz window with a radius of 15 cm. The inductive coil is excited with 13.56-MHz RF power as the source power. Further, the 2.26-MHz power and 27.12-MHz RF power are applied to the substrate as bias power. Here, argon gas pressure is 30 mTorr.

In this study, the fluid module is used to calculate the densities and fluxes of all the charged species, electron temperature, electrostatic fields, and electromagnetic fields. The plasma parameters calculated at the bulk-sheath interface based on the fluid module are used as the boundary conditions in the sheath module. The instantaneous voltage on the substrate is obtained using the sheath module, and it is employed as the boundary condition of the Poisson's equation in the fluid module. By coupling the two modules, the effects of RF bias on the plasma characteristics under different discharge conditions are accurately examined.

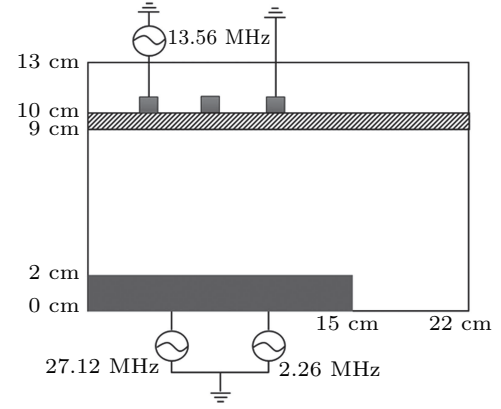


Fig. 1. Structural diagram of cylindrical ICP reactor.

2.1. Fluid module

The 2D fluid module, which has been described in earlier studies,^[17–20] is mainly composed of a plasma module and an electromagnetic module.

In the plasma module, the equations governing the dynamics of electrons are expressed as

$$\frac{\partial n_e}{\partial t} + \nabla \cdot \Gamma_e = S_e, \quad (1)$$

$$\Gamma_e = -\frac{\nabla(n_e k T_e)}{m_e v_{en}} - \frac{en_e}{m_e v_{en}} \mathbf{E}_s, \quad (2)$$

$$\frac{\partial}{\partial t} \left(\frac{3}{2} n_e k T_e \right) = -\nabla \cdot \mathbf{q}_e - e \Gamma_e \cdot \mathbf{E}_s - E_e + P_{ind}. \quad (3)$$

Here, S_e is the source term of electrons; n_e , Γ_e , T_e , m_e , and \mathbf{q}_e are the density, flux, temperature, mass, and energy flux of electrons, respectively; v_{en} is the elastic collision frequency between electrons and neutrals; \mathbf{E}_s is the electrostatic field, which is determined by solving the Poisson's equation; E_e is the energy exchange between electrons and other species in collision process; k is the Boltzmann constant; the period-averaged inductive power deposition; P_{ind} is expressed as $P_{ind} = (1/T) \int_0^T J_\theta E_\theta dt$, with J_θ and E_θ being the azimuthal electron flux and electric field, and T being the period of the power applied on the coil. Further, the azimuthal electric field is calculated by using the Maxwell's equations.

The dynamic behavior of the ions can be described from the following fluid equations:

$$\frac{\partial n_i}{\partial t} + \nabla \cdot \Gamma_i = S_i, \quad (4)$$

$$\frac{\partial n_i m_i \mathbf{u}_i}{\partial t} + \nabla \cdot (n_i m_i \mathbf{u}_i \mathbf{u}_i) = -k T_i \nabla n_i + e n_i \mathbf{E}_s + \mathbf{M}_i, \quad (5)$$

where n_i , Γ_i , m_i , and \mathbf{u}_i are the density, flux, mass, and velocity of ions, respectively. \mathbf{M}_i represents the momentum transfer from ions to neutral species by collisions.

The Poisson's equation is expressed as

$$\nabla^2 \varphi(r, z) = -\frac{e}{\epsilon_0} \left(\sum_i Z_i n_i - n_e \right). \quad (6)$$

In the electromagnetic module, the Maxwell's equations are

$$\nabla \times \mathbf{E} = -\frac{\partial \mathbf{B}}{\partial t}, \quad (7)$$

$$\nabla \times \mathbf{B} = \mu_0 \mathbf{J} + \varepsilon_0 \varepsilon_r \mu_0 \frac{\partial \mathbf{E}}{\partial t}, \quad (8)$$

where \mathbf{E} and \mathbf{B} are the time-dependent electric field and magnetic field, respectively; μ_0 and ε_r represent the vacuum permeability and the relative dielectric constant, respectively.

The equation governing the plasma current \mathbf{J} is

$$\frac{\partial \mathbf{J}}{\partial t} = \frac{n_e e^2}{m_e} \mathbf{E} - \nu_{en} \mathbf{J}, \quad (9)$$

and it is set to be zero in the regions of dielectric window and vacuum.

2.2. Sheath model

To calculate the instantaneous bias voltage at the electrode, an equivalent circuit model is presented. The sheath is considered to be a parallel combination of a diode, a capacitor, and a current source. A detailed description of this model is presented in Ref. [24]. Assuming a sinusoidal current source at the electrode, the current balance equation is

$$I_i - I_e - I_d = I_{\max} \sin(2\pi f t). \quad (10)$$

Here, I_{\max} and f are the amplitude and frequency of the current source, respectively. When dual-frequency bias power is applied to the electrode, the term on the right-hand side of Eq. (10) is modified as $I_{1\max} \sin(2\pi f_1 t) + I_{2\max} \sin(2\pi f_2 t)$, where $I_{1\max}$ and $I_{2\max}$ are the amplitudes, and f_1 and f_2 are the frequencies of the dual bias. I_i and I_e are the ion current and electron current, respectively. The capacitive displacement current I_d is expressed as

$$\begin{aligned} I_d &= \frac{dQ(t)}{dt} = \frac{dQ(t)}{dV_e(t)} \frac{dV_e(t)}{dt} \\ &= C_s(t) \frac{dV_e(t)}{dt}, \end{aligned} \quad (11)$$

where $C_s(t) = \varepsilon_0 A / d_s(t)$ and $d_s(t)$ are the sheath capacitance and sheath thickness, respectively, and ε_0 is the permittivity of free space. Based on the current balance equation, the instantaneous bias voltage at the electrode $V_e(t)$ is obtained, which is used as the boundary condition of the Poisson's equation in the bulk plasma module.

The RF bias power is given as follows:

$$P = \frac{1}{T} \int_0^T V_e(t) I(t) dt, \quad (12)$$

where $T = 1/f$ is the RF bias cycle and $I(t) = I_{\max} \sin(2\pi f t)$.

3. Results and discussion

3.1. Effect of single-frequency bias at different values of coil power

First, the 2D distributions of plasma density at different values of powers of single-frequency bias are investigated, where the frequency of the bias is fixed at 27.12 MHz. The non-uniformity degree α is defined as $\alpha = (n_{\max} - n_{\min}) / 2n_{\text{ave}}$, where n_{\max} , n_{\min} , and n_{ave} are the maximum, minimum and average plasma density along the reactor centerline from ($r = 0$ cm, $z = 5.5$ cm) to ($r = 15$ cm, $z = 5.5$ cm). Figure 2 shows that when the ICP source power is fixed at 50 W, the spatial uniformity of plasma is strongly improved (α decreases from 0.595 to 0.025) and the plasma density at the edge of the substrate significantly increases with bias power increasing. This is because when the bias power is applied, the electrons are simultaneously heated by the inductive field generated by the RF coil power and the capacitive field induced by the RF bias. Therefore, as the bias power increases from 100 W to 500 W, the electrons gain more energy from the bias deposition, which leads to a considerable increase in the plasma generation.

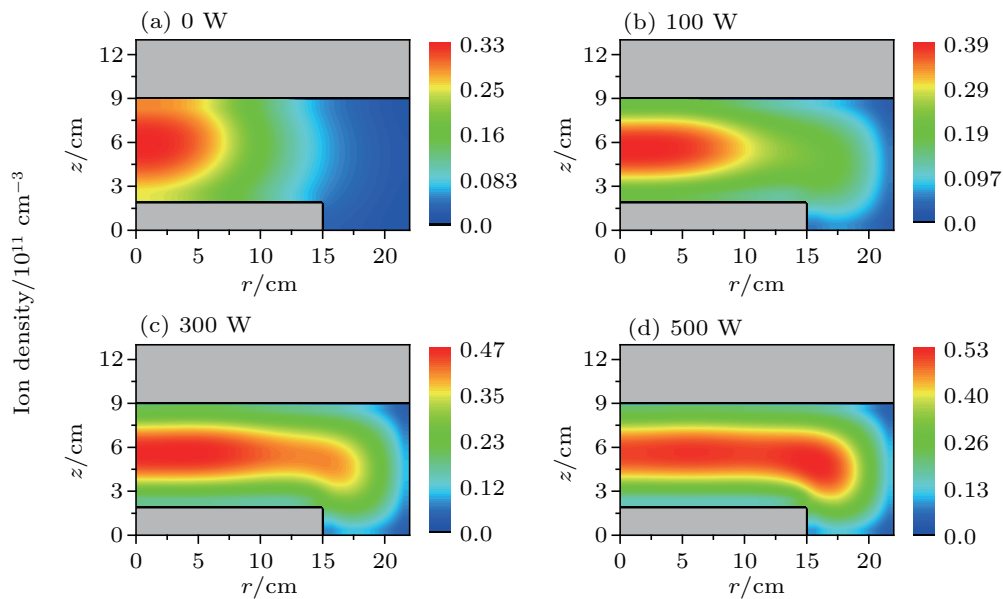


Fig. 2. Distributions of the ion density at different values of bias power: (a) 0 W, (b) 100 W, (c) 300 W, and (d) 500 W, for an argon discharge sustained at 50 W and 13.56 MHz, and bias frequency is fixed at 27.12 MHz.

As the coil power increases to 100 W, the spatial distributions of ion density including the magnitudes and shapes at various bias powers are strikingly different from those obtained at 50 W as shown in Fig. 3. Although the maximum ion density gradually shifts to the radial edge of the substrate with bias power increasing, the ion densities are characterized by a remarkable peak in the reactor center. The uniformity of plasma is extremely poor, and the plasma distribution is negligibly affected by increasing the bias power. This is be-

cause when the ICP power is high, the electric field generated by the coil significantly contributes to the plasma generation; the peak of the plasma density appears in the reactor center and cannot be mitigated by diffusion, thus enhancing plasma generation near the edge of substrate. Further, this result is consistent with that obtained in the case with low coil power (see Fig. 2), *i.e.*, the maximum plasma density moves away from the dielectric window due to the capacitive field heating caused by bias power.

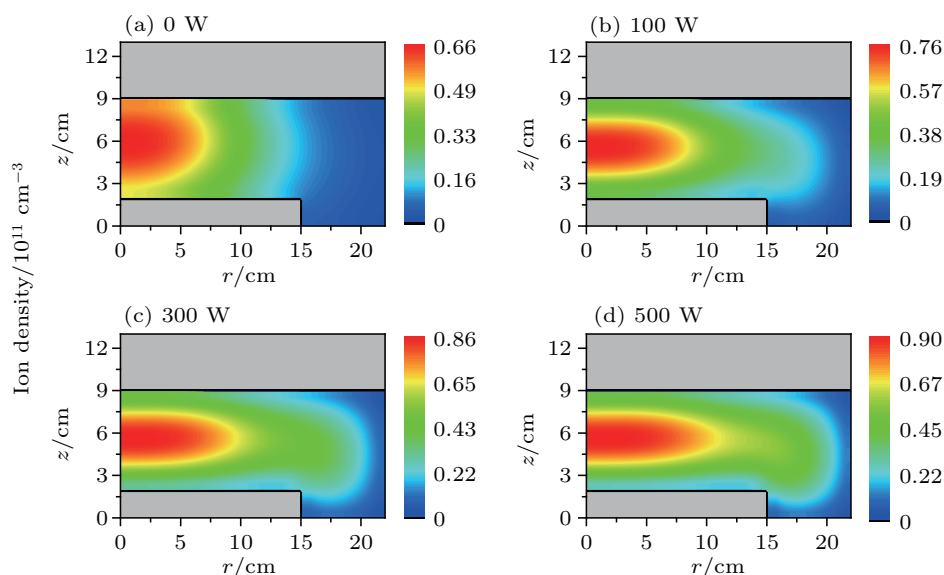


Fig. 3. Distributions of ion density at different values of bias power: (a) 0 W, (b) 100 W, (c) 300 W, and (d) 500 W, for an argon discharge sustained at 100 W and 13.56 MHz, and bias frequency is fixed at 27.12 MHz.

3.2. Effect of dual-frequency bias at different values of coil power

To further investigate the plasma characteristics in the ICP reactor simultaneously energized by ICP source power and bias power, the dependence of the source power and the dual-frequency RF bias power on the ion density is examined. The applied ICP source power is varied from 0 W to 800 W. The sum of the applied bias powers is maintained at 500 W and the ratio of 27.12-MHz/2.26-MHz bias power is controlled as follows: 0 W/500 W, 100 W/400 W, 200 W/300 W,

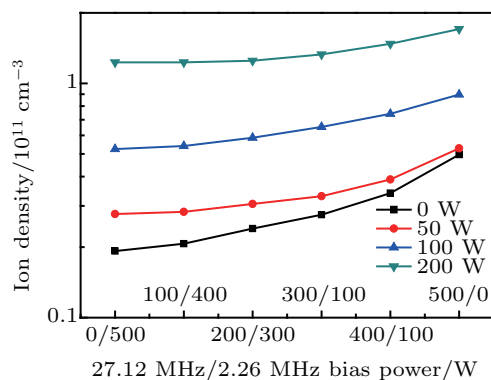


Fig. 4. Relationship between ICP source power and peak ion density for various ratios of 27.12-MHz/2.26-MHz bias power for argon discharge maintained at 100 W and 13.56 MHz.

300 W/200 W, 400 W/100 W, and 500 W/0 W. Figure 4 shows that when the ICP source power is applied, the increase in the ratio of 27.12-MHz/2.26-MHz bias power does not exhibit a significant influence on the maximum argon ion density, whereas a more pronounced increase is observed for 0-W ICP source power, which agrees well with the experimental result.^[16] Indeed, when the ICP source power is equal to 0 W, the high-frequency bias power plays a dominant role in generating the plasma.

Figures 5 and 6 show the effects of different ratios of 27.12-MHz/2.26-MHz bias power on the density profiles of argon ions for ICP source power of 50 W and 100 W, respectively. When the ICP source power is fixed at 50 W (see Fig. 5), the ion density decreases with bias power ratio decreasing, and the ion density profiles shift from edge-high to center-high as the 2.26-MHz bias power increases from 0 W to 500 W. Further, the plasma uniformity deteriorates, and the plasma non-uniformity increases from 0.025 to 0.183. This is because the electrons gain less energy from the less frequent collisions, which weakens the plasma generation near the substrate, especially at the radial edge of the substrate. This implies that the 2.26-MHz bias power has a minor effect on the spatial distribution and value of the argon ion density. As the

ICP source power further increases to 100 W (see Fig. 6), the maximum ion density slightly moves to the reactor center and becomes close to the dielectric window with the increase in the low-frequency bias power ratio. Indeed, when the source

power is higher, plasma is primarily generated by coil source power in the ICP reactor, and the plasma density is insignificantly influenced by the bias source power for different dual-bias power ratios.

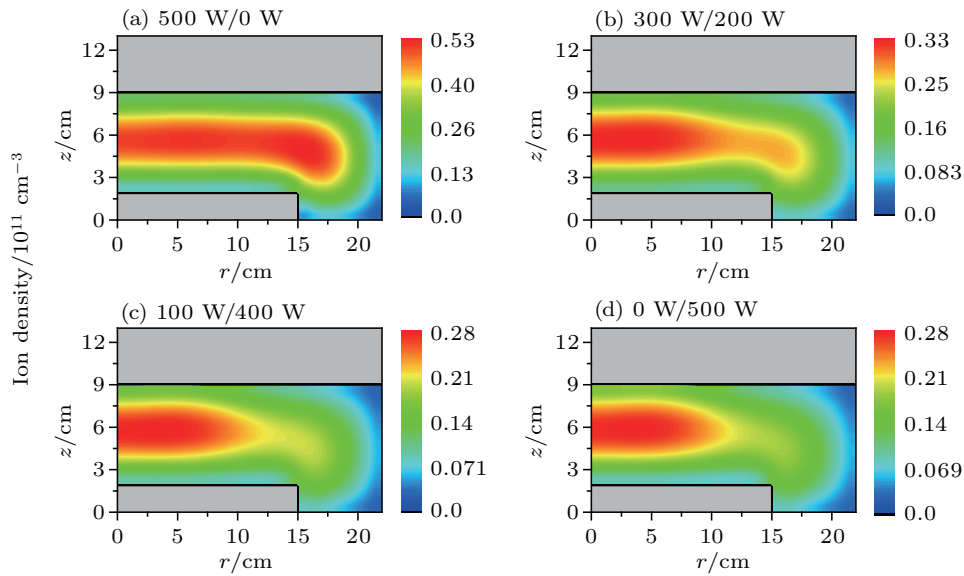


Fig. 5. Distributions of ion density at different ratios of 27.12-MHz/2.26-MHz bias powers: (a) 500 W/0 W, (b) 300 W/200 W, (c) 100 W/400 W, and (d) 0 W/500 W, for argon discharge maintained at 50 W and 13.56 MHz.

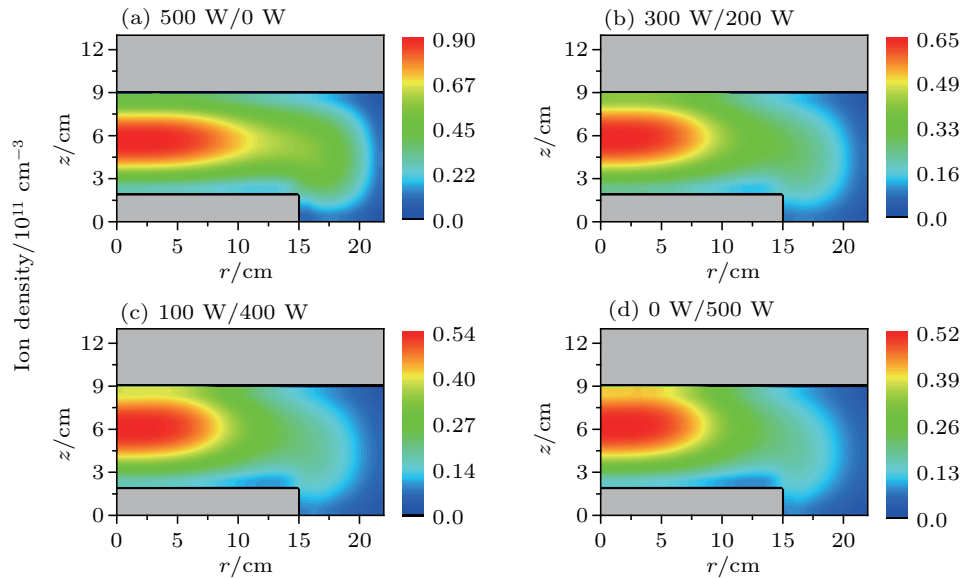


Fig. 6. Distributions of ion density at different ratios of 27.12-MHz/2.26-MHz bias power: (a) 500 W/0 W, (b) 300 W/200 W, (c) 100 W/400 W, and (d) 0 W/500 W, for argon discharge maintained at 100 W and 13.56 MHz.

The ion flux is a vital parameter for etching process. Therefore, the temporal evolution of the ion flux along the substrate surface in the range between $r = 0$ cm and $r = 15$ cm over one low-frequency bias period at different ratios of 27.12-MHz/2.26-MHz bias power for ICP source powers of 50 W and 100 W are shown in Figs. 7 and 8, respectively. In Fig. 7, the results are shown for 12 cycles at 27.12 MHz, which corresponds to 1 cycle at 2.26 MHz. When only the high-frequency bias power is applied, the absolute values of the ion flux peaks oscillate with time. The ion flux is characterized by 12 peaks

in 12 high-frequency bias periods (see Fig. 7(a)) due to the acceleration of energetic electrons by the capacitive bias field. In addition, the ion flux peak appears at the radial edge of the substrate due to the strong electric field generated by bias. When the ratio of 27.12-MHz/2.26-MHz bias power decreases to 300 W/200 W (see Fig. 7(b)) the ion flux is clearly modulated by the low-frequency power. The ion flux peaks caused by the capacitive field heating are initially remarkable in a nearly 1/4 low-frequency period, and it becomes less prominent after a nearly half period. Furthermore, a second peak

appears near the symmetry axis in an approximately 3/8 low-frequency period, which indicates that the ICP source power begins to have a stronger influence on the plasma generation. When the ratio of 27.12-MHz/2.26-MHz bias power is 100 W/400 W (see Fig. 7(c)), the modulation of the low frequency bias power becomes even more prominent. However, the oscillation of the ion flux caused by high-frequency bias

is not obvious. When the ratio of 27.12-MHz/2.26-MHz bias power is equal to 0 W/500 W, the ion flux is only modulated by low-frequency bias power, and the absolute value of the ion flux varies smoothly with time. Furthermore, a second peak in the ion flux also appears at a nearly 3/8 low frequency period. This indicates that the peak in the ion flux at the radial edge of the substrate is induced by the low-frequency bias.

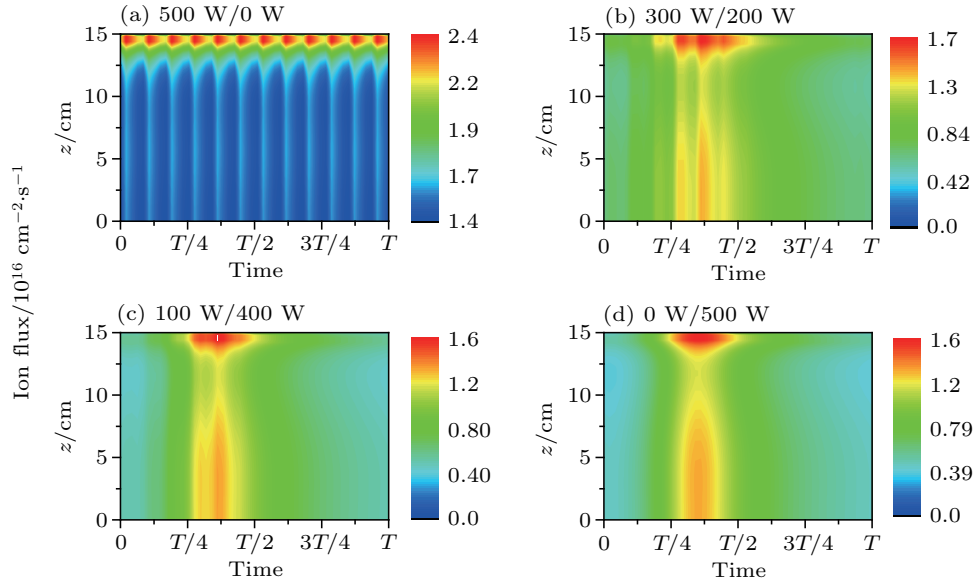


Fig. 7. Spatiotemporal distribution of ion flux along substrate surface at different ratios of 27.12-MHz/2.26-MHz bias power: (a) 500 W/0 W, (b) 300 W/200 W, (c) 100 W/400 W, and (d) 0 W/500 W, for argon discharge maintained at 50 W and 13.56 MHz.

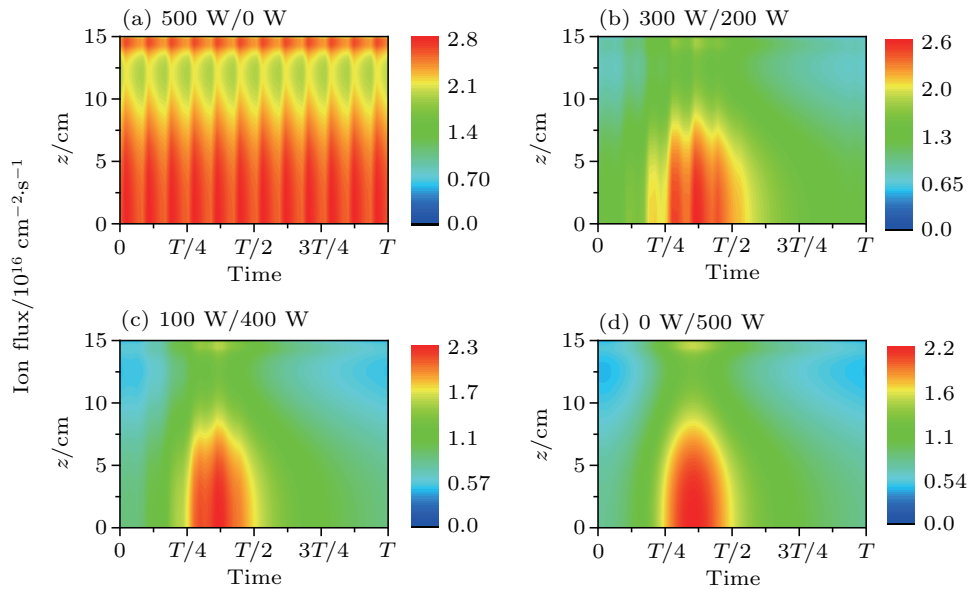


Fig. 8. Spatiotemporal distributions of ion flux along substrate surface at different ratios of 27.12-MHz/2.26-MHz bias power: (a) 500 W/0 W, (b) 300 W/200 W, (c) 100 W/400 W, and (d) 0 W/500 W, for argon discharge maintained at 100 W and 13.56 MHz.

The variation in the ion flux with the ratio of 27.12-MHz/2.26-MHz bias power for total bias power of 500 W and ICP source power of 100 W is depicted in Fig. 8. It is clear that the ion flux distributions are different from that obtained at the ICP source power of 50 W (Fig. 7). The peaks in the ion flux in the reactor center become more obvious with higher absolute values due to the enhanced generation

of plasma caused by the higher ICP source power. Indeed, in a one low-frequency period, the ion flux oscillates with a center-and-edge high profile when the ratio of 27.12-MHz/2.26-MHz bias power is 500 W/0 W (Fig. 8(a)). When the ratio of 27.12-MHz/2.26-MHz bias power decreases to 300 W/200 W and 100 W/400 W, the ion flux is maximum near the symmetry axis with higher absolute values (Figs. 8(b) and 8(c)), which

is different from the case with ICP power of 50 W (Figs. 7(b) and 7(c)). When the ratio of 27.12-MHz/2.26-MHz bias power is 0 W/500 W (Fig. 8(d)), the distribution of ion flux becomes smoother.

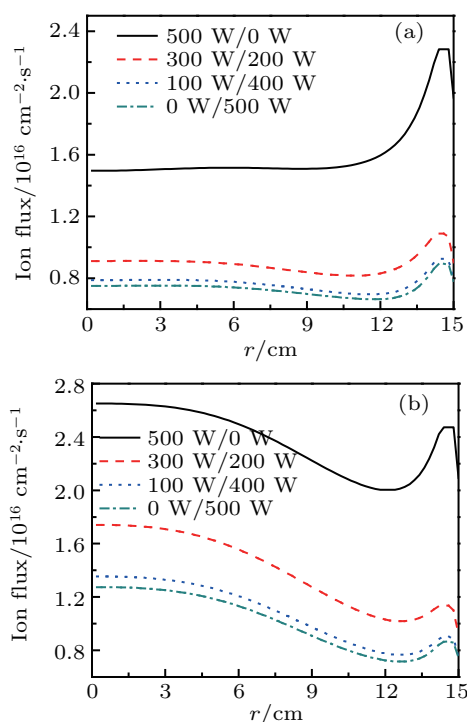


Fig. 9. Radial distributions of axial ion flux at bottom electrode averaged over one cycle of 2.26-MHz frequency, which corresponds to 12 cycles of 27.12-MHz frequency at ICP source powers: (a) 50 W and (b) 100 W, for argon discharge biased by different values of 27.12-MHz/2.26-MHz bias power, and coil frequency is fixed at 13.56 MHz.

The variations in the radial distribution of ion flux at the bottom electrode averaged over one low-frequency period with ratio of 27.12-MHz/2.26-MHz bias power for various ICP source powers are shown in Fig. 9. When the source power is 50 W (see Fig. 9(a)), the radial distribution is rather uniform in the center region until $r \approx 11$ cm and a higher absolute value is observed at the radial edge of the substrate when the bias power ratio is 500 W/0 W (*cf.* Fig. 7(a) as shown above) due to the presence of strong capacitive field. When the bias power ratio decreases to 300 W/200 W, 100 W/400 W, and 0 W/500 W, the ion fluxes exhibit edge-high profiles with a second peak in the reactor center, and the radial uniformity becomes worse (*cf.*, Fig. 7 above). Further, this also indicates that at lower ICP source power, the profile of the plasma characteristics is considerably affected by the ratio of dual-frequency bias power, and the effect of dual-frequency bias weakens with the decrease in the 27.12 MHz/2.26-MHz bias power ratio. When the source power increases to 100 W (see Fig. 9(b)) the ratio of 27.12-MHz/2.26-MHz bias power has a minor effect on radial distribution, *i.e.*, a center-and-edge high profile is observed at all the bias power ratios, which further validates that the plasma characteristic profile is negligibly affected by the dual-frequency bias power ratio at high

ICP source power. Besides, the absolute value of the ion flux exhibits an obvious decrease. This is also because the plasma generation is weakened due to the less frequent collisions, and the ion flux is lower.

Finally, figure 10 displays the radial distribution of ion flux at the bottom electrode averaged over one low-frequency cycle for different values of ICP source power where the 27.12-MHz/2.26-MHz bias power ratio is fixed at 200 W/300 W. It is clear that as the ICP source power increases, the peak of ion flux shifts from the radial edge of the substrate to the reactor center, and the value of ion flux increases with the ICP source power increasing. It is noted that the ICP source power has a significant influence on the shape and value of the ion flux. This is mainly because as the ICP source power further increases, the electrons gain more energy from the higher inductive power, and these energetic electrons enhance the ion generation near the reactor center. Thus, this again proves that when the ICP source power is high, the effect of bias power on the profile of plasma characteristic is insignificant.

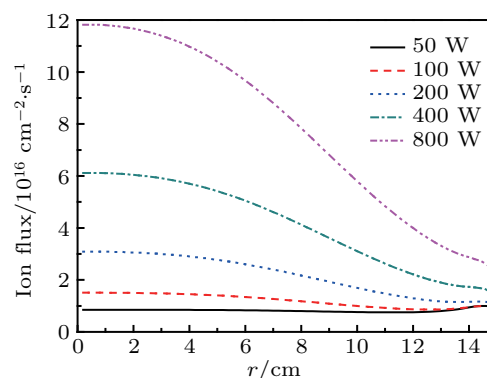


Fig. 10. Radial distributions of axial ion flux at bottom electrode averaged over one cycle for frequency of 2.26 MHz, which corresponds to 12 cycles for frequency of 27.12 MHz for different values of ICP source power in argon discharge. The 27.12-MHz/2.26-MHz bias power ratio is fixed at 200 W/300 W, and the coil frequency is set to be 13.56 MHz.

4. Conclusions

In this study, a 2D self-consistent fluid model is employed to investigate the influences of bias power on the plasma characteristics at different ICP source powers in an argon discharge. The effects of various 27.12-MHz/2.26-MHz bias powers and ICP source power are illustrated by examining the 2D distributions of plasma density and spatiotemporal distribution of ion flux as well as the radial profile of axial ion flux at the bottom electrode.

The results reveal that the bias power significantly affects the plasma characteristics at low ICP source power. When the single-frequency bias power is applied with coil power of 50 W, the effect of the bias power on the plasma characteristics becomes significant with the increase in the bias power. Accordingly, the plasma density profiles shift from center-high

to edge-high as the bias increases from 0 W to 500 W with bias frequency of 27.12 MHz, and the best plasma uniformity is obtained at 500 W. When the ICP source power increases to 100 W, the stronger inductive field produced by coil power significantly contributes to the plasma generation, and the increase in the bias power weakly affects the 2D plasma density profiles.

The effects of the ratio of 27.12-MHz/2.26-MHz bias power with total value of 500 W at various values of ICP source power on the plasma parameters are also investigated. When the ICP source power is applied, the maximum argon ion density is slightly affected by the 27.12-MHz/2.26-MHz bias power. However, when only the bias power is applied, the high-frequency bias power plays a dominant role in the plasma generation. When the ratio of 27.12-MHz/2.26-MHz bias power varies from 500 W/0 W to 0 W/500 W with the ICP source power fixed at 50 W, the plasma density profile smoothly shift from edge-high to center-high, and the best radial uniformity is obtained at 500 W/0 W. When the ICP source power is 100 W, plasma is mainly generated by coil source power, and the ratio of 27.12-MHz/2.26-MHz bias power has a weaker effect on the plasma density profile. Furthermore, the spatiotemporal distributions of the ion flux at the substrate surface over one 2.26-MHz frequency cycle are also presented. When the ICP source power is low (*e.g.*, 50 W), the ion flux is characterized by 12 peaks at the edge of the substrate for bias frequency of 27.12 MHz. When both 27.12-MHz bias power and 2.26-MHz bias power are employed, the ion flux is primarily modulated by the low-frequency power and is characterized by a center-and-edge high profile at bias power ratios of 300 W/200 W, 100 W/400 W, and 0 W/500 W. When the ICP source power increases to 100 W, the ion flux at the symmetry axis increases significantly, showing obvious maxima at all the selected ratios of dual-frequency bias power. The radial distribution of ion flux at the bottom electrode averaged over one low bias frequency is also investigated. When the ICP source power is fixed at 50 W, the axial ion flux exhibits a maximum at the radial edge of the substrate. When the ICP source power is higher than 50 W, the axial ion flux is characterized by a maximum in the reactor center with a second peak at the radial edge of the substrate for all selected

discharge conditions.

Overall, we confirm that low-frequency bias has a weaker effect on plasma distribution than high-frequency bias, and the spatial distribution of plasma characteristics can be controlled by changing the bias power of a single-frequency bias or high-frequency bias power ratio of dual-frequency bias, especially at low ICP source power, which is favorable for optimizing the etching process.

References

- [1] Efremov A, Min N K, Jeong J, Kim Y and Kwon K 2010 *Plasma Sources Sci. Technol.* **19** 045020
- [2] Li J S, Wang J X, Yin M, Gao P Q, He D Y, Chen Q, Li Y L and Shirai H 2008 *J. Appl. Phys.* **103** 043505
- [3] Qin S and McTeer A 2007 *Surf. Coat. Technol.* **201** 6759
- [4] Lee H C, Bang J Y and Chung C W 2011 *Thin Solid Films* **519** 7009
- [5] Lee H C, Oh S J and Chung C W 2012 *Plasma Sources Sci. Technol.* **21** 035003
- [6] Sobolewski M A and Kim J H 2007 *J. Appl. Phys.* **102** 113302
- [7] Ahr P, Schüngel E, Schulze J, Tsankov Ts V and Czarnetzki U 2015 *Plasma Sources Sci. Technol.* **24** 044006
- [8] Schulze J, Schüngel E and Czarnetzki U 2012 *Appl. Phys. Lett.* **100** 024102
- [9] Zaka-ul-Islam M, O'Connell D, Graham W G and Gans T 2015 *Plasma Sources Sci. Technol.* **24** 044007
- [10] Hoekstra R J and Kushner M J 1996 *J. Appl. Phys.* **79** 2275
- [11] Takekida H and Nanbu K 2005 *J. Phys. D: Appl. Phys.* **38** 3461
- [12] Tinck S, Boullart W and Bogaerts A 2008 *J. Phys. D: Appl. Phys.* **41** 065207
- [13] Kwon D C, Chang W S, Park M, You D H, Song M Y, You S J, Im Y H and Yoon J S 2011 *J. Appl. Phys.* **109** 073311
- [14] Gao F, Zhang Y R, Zhao S X, Li X C and Wang Y N 2014 *Chin. Phys. B* **23** 115202
- [15] Han C K, Yang Y Y, Liu W F, Lu Y J and Cheng J 2018 *SPIN* **8** 1850002
- [16] Jang H and Chae H 2017 *Nano* **12** 1750025
- [17] Si X J, Zhao S X, Xu X, Bogaerts A and Wang Y N 2011 *Phys. Plasmas* **18** 033504
- [18] Sun X Y, Zhang Y R, Li X C and Wang Y N 2015 *Phys. Plasmas* **22** 053508
- [19] Sun X Y, Zhang Y R, Li X C and Wang Y N 2017 *Chin. Phys. B* **26** 015201
- [20] Sun X Y, Zhang Y R, Chai S, Wang Y N and He J X 2019 *Phys. Plasmas* **26** 043503
- [21] Wang Y H, Liu W, Zhang Y R and Wang Y N 2015 *Chin. Phys. B* **24** 095203
- [22] Zhang Y R, Gao F, Li X C, Bogaerts A and Wang Y N 2015 *J. Vac. Sci. Technol. A* **33** 061303
- [23] Zhang Y R, Zhao Z Z, Xue C, Gao F and Wang Y N 2019 *J. Phys. D: Appl. Phys.* **52** 295204
- [24] Edelberg E A and Aydil E S 1999 *J. Appl. Phys.* **86** 4799